



This is a repository copy of *Self-healing WS2 tribofilms: An in-situ appraisal of mechanisms*.

White Rose Research Online URL for this paper:  
<https://eprints.whiterose.ac.uk/178471/>

Version: Published Version

---

**Article:**

Cao, H., Bai, M., Inkson, B.J. [orcid.org/0000-0002-2631-9090](https://orcid.org/0000-0002-2631-9090) et al. (4 more authors)  
(2021) Self-healing WS2 tribofilms: An in-situ appraisal of mechanisms. *Scripta Materialia*,  
204. 114124. ISSN 1359-6462

<https://doi.org/10.1016/j.scriptamat.2021.114124>

---

**Reuse**

This article is distributed under the terms of the Creative Commons Attribution (CC BY) licence. This licence allows you to distribute, remix, tweak, and build upon the work, even commercially, as long as you credit the authors for the original work. More information and the full terms of the licence here:  
<https://creativecommons.org/licenses/>

**Takedown**

If you consider content in White Rose Research Online to be in breach of UK law, please notify us by emailing [eprints@whiterose.ac.uk](mailto:eprints@whiterose.ac.uk) including the URL of the record and the reason for the withdrawal request.



[eprints@whiterose.ac.uk](mailto:eprints@whiterose.ac.uk)  
<https://eprints.whiterose.ac.uk/>



## Self-healing WS<sub>2</sub> tribofilms: An *in-situ* appraisal of mechanisms

Huatang Cao<sup>a,\*</sup>, Mingwen Bai<sup>b,e</sup>, Beverley J Inkson<sup>b</sup>, Xiangli Zhong<sup>a</sup>, Jeff Th.M. De Hosson<sup>c</sup>, Yutao Pei<sup>d</sup>, Ping Xiao<sup>a,\*</sup>

<sup>a</sup> Henry Royce Institute, Department of Materials, University of Manchester, Manchester M13 9PL, UK

<sup>b</sup> Department of Materials Science and Engineering, University of Sheffield, Sheffield S1 3JD, UK

<sup>c</sup> Zernike Institute for Advanced Materials, University of Groningen, Groningen 9747AG, The Netherlands

<sup>d</sup> Engineering and Technology Institute Groningen, University of Groningen, Groningen 9747AG, The Netherlands

<sup>e</sup> Institute for Future Transport & Cities, Coventry University, Coventry CV1 5FB, UK

### ARTICLE INFO

#### Article history:

Received 1 May 2021

Revised 30 June 2021

Accepted 2 July 2021

Available online 31 July 2021

#### Keywords:

*In-situ* Microscopy

Self-healing

WS<sub>2</sub> atomic arrangement

Intelligent coating

Tribology

### ABSTRACT

Self-healing tribocoatings are being developed for aerospace applications to improve the lifetime and reduce the surface maintenance of components in motion. Here the tribo-induced self-healing behaviour of a WS<sub>2</sub>/a-C tribocoating has been evaluated for the first time by *in-situ* scanning electron microscopy (SEM) to evaluate the mechanisms of damage and self-recovery. *In-situ* SEM imaging reveals that scratch damage results in coating brittle fracture and spalling, and that Hertzian pressure affects healing rate at early stages of sliding. WS<sub>2</sub> nanocrystallites, formed via atomic rearrangement at flexural interfaces, enable the healing of irregular damages and congruently offer superlubrication in vacuum. Such damage control in tribo-service may make flawless coatings an unnecessary prerequisite in tribo-applications.

© 2021 The Author(s). Published by Elsevier Ltd on behalf of Acta Materialia Inc.

This is an open access article under the CC BY license (<http://creativecommons.org/licenses/by/4.0/>)

The development of self-healing tribocoatings for use in extreme conditions in aerospace has great potential to stabilize surface component functionality, repair damage, minimize maintenance and prolong lifetimes [1,2].

Layered WS<sub>2</sub> is well known for its excellent solid lubrication in the aerospace industry due to its highly anisotropic trigonal prismatic structure [3,4], with each unit consisting of a layer of W atoms sandwiched between two layers of hexagonally stacked sulphur atoms. The low shear strength along the WS<sub>2</sub> basal (002) orientation allows easy basal glides and results in ultralow friction [3]. To exploit the lubricating properties of WS<sub>2</sub>, WS<sub>2</sub> can be incorporated into lubricants, coatings, and composites [5], or formed *in-situ* from the wear of W-S containing materials [6]. Previous studies have demonstrated that soft crystalline WS<sub>2</sub> can be selectively released from a hard nanocomposite bulk [6,7], forming a WS<sub>2</sub>-dominated tribofilm covering the wear track and generating a transfer film on the sliding counterpart. The intrinsic frictional property of WS<sub>2</sub> inspires us to exploit a likewise self-healing capability of W-S containing coating: during tribo-service WS<sub>2</sub> forms tribofilm that itself seals potential complex-shaped damages flexibly [6]. The origin damage self-healing mechanism, particularly at

its early stages is, however, not yet clear due to the lack of a real-time characterization tool. Here, novel scratching/tribotest experiments were performed via *in-situ* SEM, which enables concurrent imaging and assessment of the local damage, wear, tribofilm generation and surface self-recovery. It is also noteworthy that SEM provides an ideal *vacuo* environment (although not ultra-high vacuum (UHV) still at 10<sup>-6</sup> mbar) enables to explore the self-healing potential of a tribocoating in mimicked aerospace conditions.

Nanocomposite WS<sub>2</sub>/a-C coatings were deposited on single crystal silicon (100) wafers via a TEER UDP400/4 closed-field unbalanced magnetron sputtering system (CFUMS). The substrates were ultrasonically cleaned in acetone prior to Ar plasma etching for 20 min at a negative bias voltage of 400 V (p-DC at 250 kHz). The nanocomposite coatings were co-sputtered from two WS<sub>2</sub> targets (99.9% purity) at a current of 0.5A (p-DC at 150 kHz) and one graphite target (99.9% purity, 0.5 A, DC). The substrates were located vertically onto a carousel holder with a rotation speed of 3 rpm in front of the targets. A ~1.6 μm thick WS<sub>2</sub>/a-C coating was deposited in an Ar deposition pressure of 0.6 Pa on the top of 300 nm thick Cr interlayer. The coating consists of < 5 nm WS<sub>2</sub> nanoplatelets embedded in an amorphous carbon matrix and has a hardness of 6–7 GPa. The coating microstructure was described in detail elsewhere [8,9].

In this study, an *in-situ* nano-indenter system (Alemnis AG, Thun, Switzerland) equipped with a 60° conical diamond tip

\* Corresponding authors.

E-mail addresses: [huatang.cao@manchester.ac.uk](mailto:huatang.cao@manchester.ac.uk) (H. Cao), [p.xiao@manchester.ac.uk](mailto:p.xiao@manchester.ac.uk) (P. Xiao).

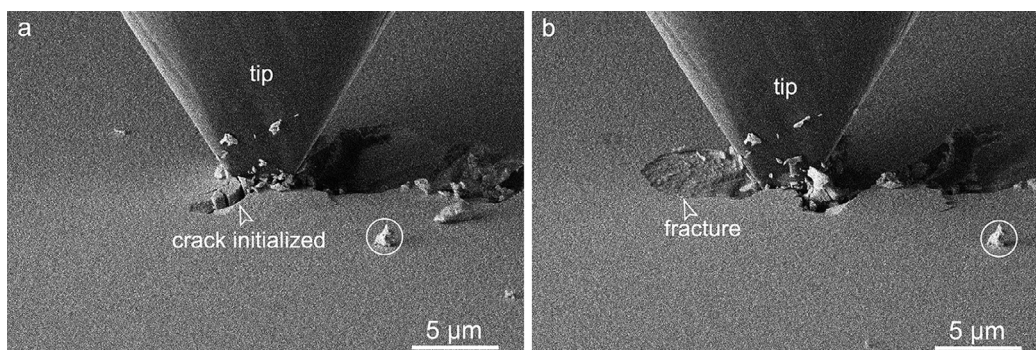


**Fig. 1.** (a) *In-situ* SEM examination of typical scratch induced surface damage of the  $WS_2/a-C$  coating (a) crack initialized (b) lateral conchoidal fracture and spalling. Typical videos recording the *in-situ* scratching are enclosed in Fig. S1a-b Supplementary Information. The circle in (a, b) is an *in-situ* reference.

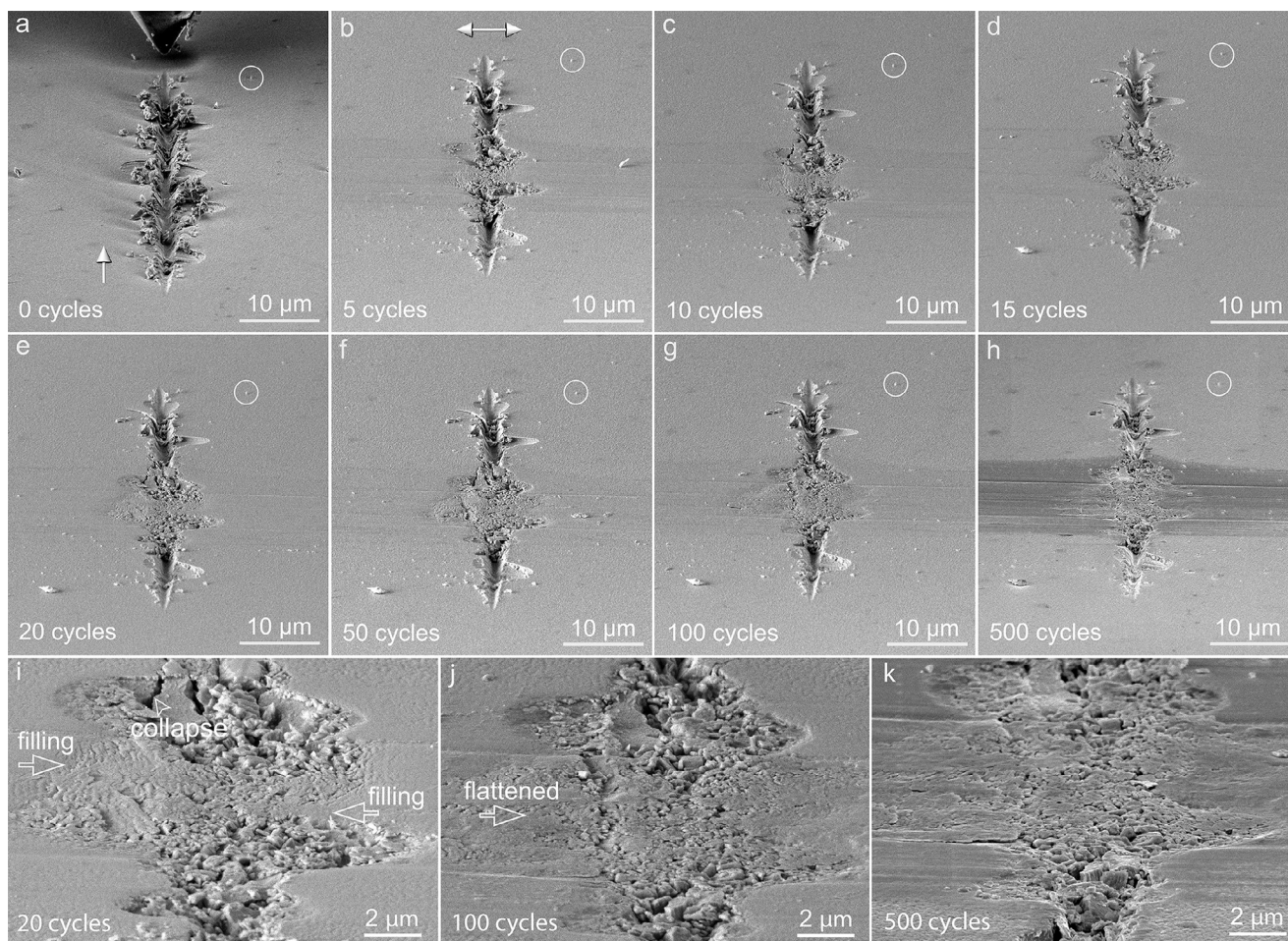


**Fig. 2.** (a) Initial scratch of  $WS_2/a-C$  nanocomposite coating. (b-h) *In-situ* SEM examination of partial healing process of the scratch damage by indicated 0-500 reciprocating sliding cycles, under a normal load of 250 mN. (i, j, k) higher magnification images of the healed scratch in (e, g, h). The arrows in (a, b) indicate the scratching/reciprocating rubbing directions. The circle in (a-h) is an *in-situ* reference. A video recording the *in-situ* healing process is enclosed in Fig. S1c Supplementary Information.

(tip diameter  $0.7 \mu\text{m}$ , SYNTON-MDP AG, Switzerland) was used inside a FEG-SEM (FEI, Nova NanoSEM 450) to locally induce cracks/damage on the surface of the coating by scratching (25 mN load), which is illustrated in the Supplementary video of Fig. S1a-b. A piezoelectric transducer (“SmartTip” Alemnis AG) was used to measure the 3-axis dynamic forces, including both the normal ( $z$ ) and lateral forces ( $x, y$ ) during the *in-situ* tests (see Fig. S2b).

Afterward, micro-tribotests were conducted in the same SEM to trigger self-repair of the damage. Specifically, a SiC sphere (diameter  $800 \mu\text{m}$ , G16, elastic modulus 410 GPa and Poisson’s ratio 0.14, Bearing Warehouse Ltd, UK) was rubbed across chosen scratches,

perpendicular (at  $90^\circ$ ) to the original scratch direction. Two wear tests, with different normal loads of 250 mN and 500 mN, were carried out across the scratches on the coating in a reciprocal sliding movement of  $100 \mu\text{m}$  stroke length at a frequency of 0.5Hz ( $100 \mu\text{m/s}$ ), producing mean Hertzian pressures of around 1.0 GPa and 1.4 GPa on the coating, respectively.

Supplementary video of Fig. S1c demonstrates the *in-situ* dynamical tribo-induced healing process of the  $WS_2/a-C$  coating. To evaluate the efficiency at the early stages of healing process, the tribotest was interrupted at 5, 10, 15, 20, 50, 100 and up to 500 reciprocating sliding cycles, respectively, for *in-situ* SEM microscopic

characterization. Transmission electron microscopy (TEM) was conducted by JEOL 2010 F (200 kV).

Fig. 1 shows a side-view of the scratch induced damage in the coating. Fig. 1a indicates the tip introduces the cracks during the ploughing and Fig. 1b shows the generation of lateral cracks result in conchoidal brittle fracture, leading to spalling up to distance a few microns from a relatively deep central groove (see the videos in Fig. S1-2). Additionally, some scratch debris is pushed to the side, up the tip, and ejected up to  $\sim 5 \mu\text{m}$  from the central groove. Figs. 2a (a close-view shown in Fig. S2a) and 3a both show the scratch damage and spallation of variable width up to around  $10 \mu\text{m}$ . At the scratch centre, a conical-shaped groove is around  $1.8 \mu\text{m}$  deep (tip displacement shown in Fig. S2b) and  $1.7 \mu\text{m}$  wide (see Fig. S2a), indicating that the damage penetrates through the whole coating into the Si substrate. Note that each conchoidal fracture event during scratching is associated with both normal and lateral force drops (marked A-E in Fig. S2).

Considering the microstructural evolution of the scratch damage, initiated by the perpendicular sliding of a SiC ball at 250 mN normal load, Fig. 2b shows that after sliding of 5 cycles the scratch debris scattered on the surface shown in Fig. 2a has been slipped away by the ball (see sliding process in Fig. S1c video) and some of the debris are refilled into the central part of the scratch. After 10-20 cycles (Figs. 2(c-e, i)), there is further gradual compaction of

debris into both the central scratch, and the surrounding sites of conchoidal fracture and spallation.

After sliding to 50 and 100 cycles (Fig. 2(f, g, j)), there is no more material from the original scratch debris filled into the scratch, but the perpendicular wear track becomes gradually deeper when compared to Fig. 2b. After 500 cycles, the wear track becomes more apparent, with some shallow perpendicular grooving (Fig. 2h) (around  $10 \mu\text{m}$  wide). Fig. 2i-k are close-up images of the wear track after sliding 20, 100 and 500 cycles, respectively; it is noteworthy that although at the early stages of healing some further collapse of previous conchoidal fracture after scratch occurs at the edge of the scratch (see Fig. 2i), the scratch damages/cracks do not induce further severe coating delamination or spalling failures under the subjected sliding pressure. Instead, Figs. 2h-j indicate that new wear debris by SiC lateral sliding are further filling into the scratch track, and flatten after 100 cycles. Nevertheless, the central healed part is still rather loose, even with several new cracks forming within the surface tribofilm due to dynamical displacement or splitting of the debris (Fig. 2k), indicating that the scratch damages are only partially healed after 500 sliding cycles under a low load of 250 mN.

In contrast, Fig. 3 shows that using perpendicular sliding under a higher applied load of 500 mN, scratch damage in the  $\text{WS}_2/\text{a-C}$  coating can be healed at a faster rate. 5 cycles of sliding at 500

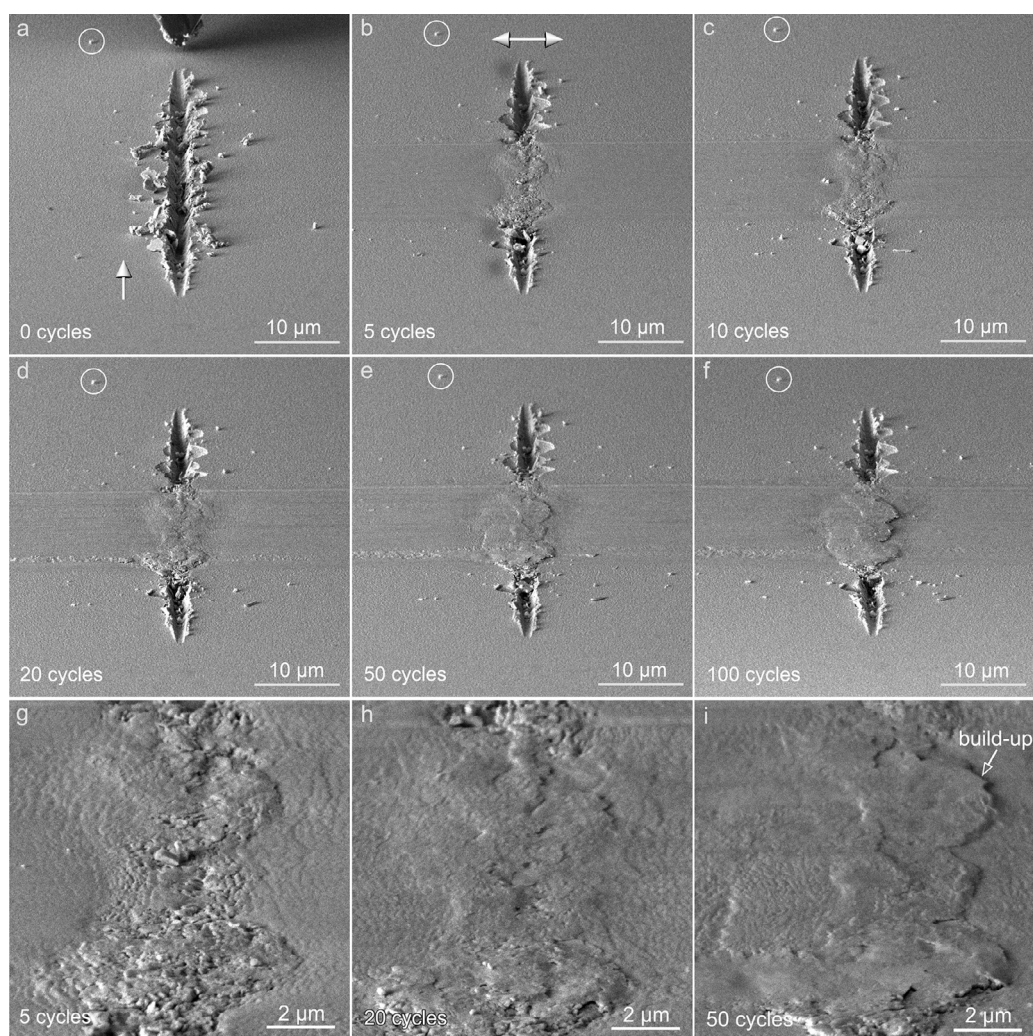
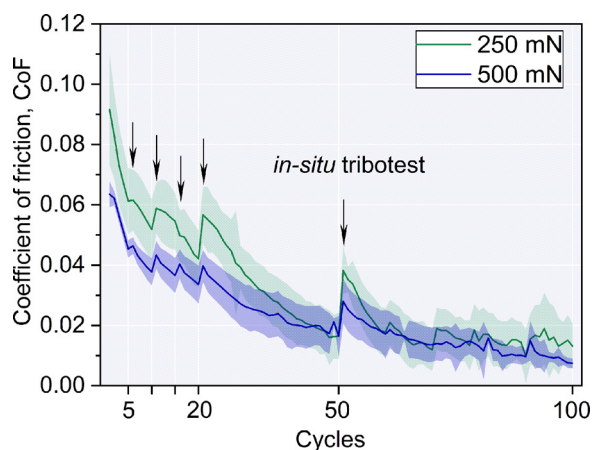


Fig. 3. (a) Initial scratch of  $\text{WS}_2/\text{a-C}$  nanocomposite coating. (b-f) *In-situ* SEM examination of the partial healing process of the scratch damage by indicated 0-100 reciprocating sliding cycles, under a higher normal load of 500 mN. The arrows in (a, b) indicate the scratching/reciprocating rubbing directions. (g, h, i) higher magnification images of the healed scratch in (b, d, e). The circle in (a-f) is an *in-situ* reference.



**Fig. 4.** Decreasing average CoF at accumulated periodic sliding cycles under normal loads of 250 mN and 500 mN. Note that the CoFs are calculated using the lateral force along the wear track axis. Each sliding re-start (after SEM imaging) generates a short running-in phase with a minor increase in CoF.

mN (Fig. 3b and g) already yield an almost complete ‘patch’ bridging the scratch. After 20 cycles (Fig. 3d and h), the edge conchoidal fracture of the scratch is sufficiently flattened, and the new central plug is compact without observable porosities. After 50 cycles (Fig. 3e and i), there is an accumulated build-up of tribofilm compactly covering the scratch damage, justifying an effective repair.

For the as-deposited WS<sub>2</sub>/a-C coating, during the sliding process, the surface asperities of the dome-like coating (Fig. S3a) are first truncated by SiC ball sliding (Fig. S3b), and the resulting wear debris (main healing agent) are continuously transformed into tribofilms and pushed to infill the micro-valleys and potentially larger scratch cracks/damages, leading to a gradually flat and highly smoothed surface particularly under a higher sliding pressure (compare Fig. S3b with Fig. S3c).

To examine further the perpendicular sliding and healing process, the average coefficient of friction (CoF) for up to 100 cycles of reciprocating sliding was calculated using the lateral force along the sliding direction (similar to that in Fig. S2b). The CoF is load-dependent, and the higher 500 mN normal load yields a lower CoF compared to 250mN, which is a typical characteristic of WS<sub>2</sub> based tribocoating [10]. Under both loads, the CoF decreases with increasing cycles, reaching 0.02 at 50 cycles and < 0.01 (a superlubricity state) around after 100 sliding cycles for 250 mN and 500 mN, respectively. It should be noted that there are some spatial spikes of friction on the damaged areas of the wear track (not shown). The friction spikes and average CoF decrease because of the gradual tribofilm formation and better repair of scratch damage. A higher load builds up the tribofilm and smoothens the scratch faster, resulting in both a lower average CoF and an earlier

arrival at superlubricity. Such low CoFs of the WS<sub>2</sub>/a-C nanocomposite coating fully fulfil the criteria of solid lubricating coatings for aerospace applications (CoF < 0.1 as proposed [4]).

Under cyclic sliding, wear debris is pushed into scratch damage locations, and originally loose debris become compacted and transformed into tribofilms to heal the damage completely. Our earlier study on the same coating *ex-situ* healed under dry air conditions [6] showed that along the side flexural surface of the damage, WS<sub>2</sub> nanocrystallites are reorientated via atomic rearrangement (Fig. 5a) and spread conformally with the damage interface (see dash line in Fig. 5a and marker in Fig. 5b), contrasting with the originally randomly oriented WS<sub>2</sub> lamina in the bottom coating (see Fig. 5a).

This WS<sub>2</sub> synchronic reorientation may be enhanced with a higher Hertzian pressure (1.0 GPa→1.4 GPa): higher local interfacial forces could lead to a higher interfacial commensurability (as verified by Fig. 3h in comparison to Fig. 2i for both 20 cycles under two loads), similar to the frictional contact of graphene [11]. Meanwhile, under vacuum sliding WS<sub>2</sub> nanocrystallites in the tribofilm over the wear track and healed scratch can also be favourably re-aligned with their (002) basal planes straight parallel to the ball sliding direction congruently offering superlubricity (CoF < 0.01) as confirmed in Fig. 4.

On the one hand, the increase of coating hardness to 6-7 GPa via incorporating an amorphous carbon matrix to embed WS<sub>2</sub> (< 0.5 GPa for pure WS<sub>2</sub> [9]) introduces brittleness to the nanocomposite when suffering scratching (Fig. S1-2); on the other hand, with the cushion support from the hard fractured surface of the bottom coating and the direct squeeze from top SiC ball (20-30 GPa), intrinsically soft WS<sub>2</sub> are released out from WS<sub>2</sub>/a-C bulk/wear debris and are subsequently re-arranged via stacking faults [12] under local shear, rendering their (002) basal planes to extend flexibly (see Fig. S4) to heal irregular damage even with brittle fractures (flexible configuration forming a synchronic closure loop as shown in the schematic of Fig. 5b).

The first *in-situ* SEM evaluation of the scratch damage and self-healing behaviour of a WS<sub>2</sub>/a-C nanocomposite coating has been carried out. *In-situ* scratching with a sharp tip reveals that the pristine WS<sub>2</sub>/a-C coating deforms by predominantly brittle failures, with conchoidal fractures and spalling. Surface abrasion initiates surface self-healing of the scratch damage by tribofilms: WS<sub>2</sub> nanocrystallites are re-arranged from bulk coating/refilled debris and pave conformally along the flexural surface of the complex-shaped damage. It is found that a higher Hertzian contact pressure promotes a higher healing rate as formed tribofilms ‘patch’ the damage more compactly: a continuously smooth surface is generated after sliding only 20 cycles under ~1.4 GPa pressure.

The WS<sub>2</sub>/a-C coating is demonstrated to exhibit both intrinsically self-healing and superlubricity (CoF < 0.01) on tribofilm formation in vacuum conditions. The coating damage tolerance and

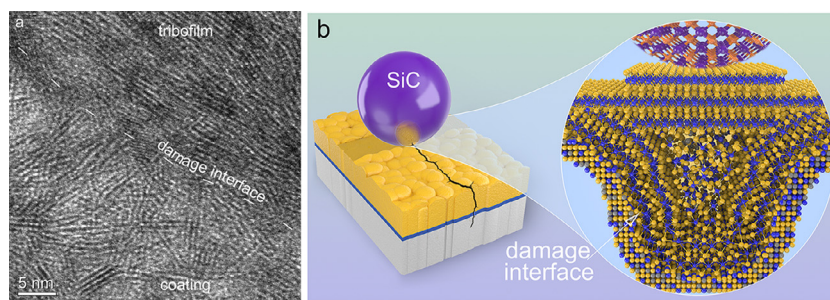


**Fig. 5.** (a) HR-TEM image of flexibly re-arranged WS<sub>2</sub> along the flexural surface and as a consequence healing irregular damages without any voids/cavities left (the dash line plots the interface of the damage) under dry air sliding [6]; (b) schematic illustration (not to scale) of flexible WS<sub>2</sub> tribofilms transformed from the pristine coating/debris bringing about damage-healing and offering lubrication (the coloured atoms in the magnified image: blue-W, yellow-S, grey-C).

self-healing potential may relax the necessity of producing flawless tribocoatings for aerospace triboapplications as tribo-induced self-healing initiates once damage occurs.

### Declaration of Competing Interest

The authors declare that they have no known competing financial interests or personal relationships that could have appeared to influence the work reported in this paper.

### Acknowledgment

The WS<sub>2</sub>/a-C nanocomposite coating was deposited at University of Groningen, the Netherlands. M.W.B. and B.J.I. acknowledged the Engineering and Physical Sciences Research Council (EPSRC) for the program grant EP/R001766/1 as a part of 'Friction: The Tribology Enigma'. P.X. acknowledged Royal Academy of Engineering and Rolls-Royce for appointment of Rolls-Royce/Royal Academy of Engineering Research Chair in Advanced Coating Technology. The authors are grateful for the Henry Royce Institute for Advanced Materials, funded through EPSRC grants EP/R00661X/1, EP/S019367/1, EP/P025021/1 and EP/P025498/1.

### Supplementary materials

Supplementary material associated with this article can be found, in the online version, at [doi:10.1016/j.scriptamat.2021.114124](https://doi.org/10.1016/j.scriptamat.2021.114124).

### References

- [1] B.M.D. Hager, P. Greil, C. Leyens, S.V. Der Zwaag, U.S. Schubert, *Adv. Mater.* 22 (2010) 5424–5430.
- [2] H.J. Gong, C.C. Yu, L. Zhang, G.X. Xie, D. Guo, J.B. Luo, *Compos. B: Eng.* 202 (2020) 108450.
- [3] S. Prasad, J. Zabinski, *Nature* 387 (1997) 761–763.
- [4] A.A. Voevodin, J.S. Zabinski, *Compos. Sci. Technol.* 65 (2005) 741–748.
- [5] F. Gustavsson, S. Jacobson, *Tribol. Int.* 101 (2016) 340–347.
- [6] H.T. Cao, J.T.M. De Hosson, Y.T. Pei, *Mater. Res. Lett.* 7 (3) (2019) 103–109.
- [7] L. Isaeva, J. Sundberg, S. Mukherjee, C.J. Pelliccione, A. Lindblad, C.U. Segre, U. Jansson, D.D. Sarma, *Acta Mater.* 82 (2015) 84–93.
- [8] H.T. Cao, F. Wen, S. Kumar, P. Rudolf, J.T.M. De Hosson, Y.T. Pei, *Surf. Coat. Technol.* 365 (2019) 41–51.
- [9] H.T. Cao, J.T.M. De Hosson, Y.T. Pei, *Surf. Coat. Technol.* 332 (2017) 142–152.
- [10] T. Polcar, M. Evaristo, A. Cavaleiro, *Plasma Process. Polym.* 6 (2009) 417–424.
- [11] S.Z. Li, Q.Y. Li, R.W. Carpick, P. Gumbsch, X.Z. Liu, X.D. Ding, J. Sun, J. Li, *Nature* 539 (2016) 541–546.
- [12] H.T. Cao, J. Momand, A. Syari'ati, F. Wen, P. Rudolf, P. Xiao, J.T.M. De Hosson, Y.T. Pei, *ACS Appl. Mater. Interfaces* 13 (2021) 28843–28854.